Atomic Spectroscopy

Article

Covalent Targeting Drug Mediated Specific Lanthanide Tagging Towards In Situ Bruton's Tyrosine Kinase Quantification Using ICP-MS

Ruxue Hou,[a,†] Yuxin Gu,[a,†] Yang Zhao,[a] Xinyue Zhao,[a] Limin Yang,[a] Xiaowen Yan,[a,b,*] and Qiuquan Wang [a]

[a] Department of Chemistry and the MOE Key Laboratory of Spectrochemical Analysis & Instrumentation, College of Chemistry and Chemical Engineering, Xiamen University, Xiamen 361005, P. R. China

[b] Innovation Laboratory for Sciences and Technologies of Energy Materials of Fujian Province (IKKEM), Xiamen 361005, P. R. China

Received: *April 03, 2024;* ***Revised:*** *April 23, 2024;* ***Accepted:*** *May 02, 2024;* ***Available online:*** *May 02, 2024.*

DOI: 10.46770/AS.2024.078

ABSTRACT: Bruton's tyrosine kinase (BTK) is an important target for the treatment of multiple B-cell malignancies and autoimmune diseases. Development of approach that can accurately detect the expression and activity of BTK in live cells is of great significance for the diagnosis and treatment of cancer. In this study, we exploited ibrutinib, an FDA approved covalent targeting drug, for specific lanthanide labeling and quantification of BTK in live Ramos Burkitt's lymphoma cells. A Europium (Eu) labeled ibrutinib probe (Ibt-DOTA-Eu) probe was first synthesized by conjugation of ibrutinib with DOTA, a chelator which can form highly stable complexes with lanthanides. We found that Ibt-DOTA-Eu is difficult to penetrate the cell membrane for in situ BTK labeling. To overcome this problem, we designed and synthesized an azide-modified ibrutinib probe (Ibt-N_3) that can easily pass through the cell membrane, label BTK in live cells, and then realize DBCO-DOTA-Eu labeling through strain-promoted azide-alkyne cycloaddition (SPAAC) reaction. The Eu-labeled BTK in Ramos cells is quantified to be 61.28 ng/10^6 cells by using ^{153}Eu-species-nonspecific-isotope-dilution ICP-MS coupled with HPLC. To our knowledge, this is the first study quantifying a disease-relevant kinase in live cells by using covalent targeting drug mediated lanthanide labeling and ICP-MS, which will prompt the application of ICP-MS in disease diagnosis and drug development in the future.

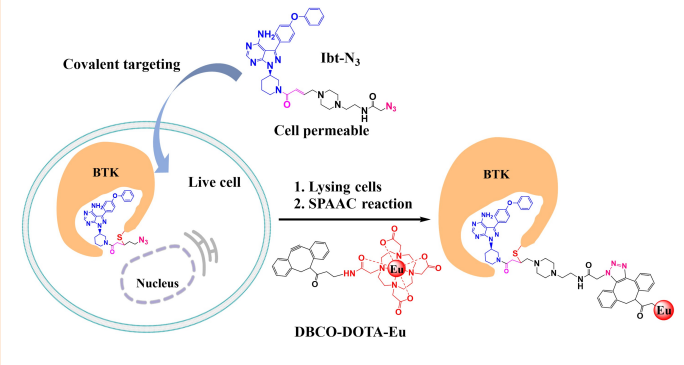

INTRODUCTION

Bruton's tyrosine kinase (BTK), a member of the Tec family of non-receptor tyrosine kinases, plays an important role in the B cell receptor (BCR) signaling pathway.[1,2] As a protein crucial for B cell development, maturation and signaling, BTK is tightly regulated in cells.[3] Abnormal expression of BTK is found disturbing the BCR signaling pathway,[4,5] leading to pathogenesis of B cell lymphoma. Research has shown that BTK is overexpressed in several B cell malignancies,[6] such as chronic lymphocytic leukemia (CLL), mantle cell lymphoma (MCL), diffuse large B-cell lymphoma (DLBCL) and acute myeloid leukemia (AML).[7,8] Additionally, a number of autoimmune diseases such as rheumatoid arthritis,[9] systemic lupus erythematosus and multiple sclerosis,[10] are also implicated in abnormal BTK expression levels. Therefore, accurately quantifying the expression and activity of BTK in live cells is of great significance for the diagnosis and treatment of these disease.

Several approaches have been developed for BTK detection.[10-15] For example, Honigberg *et al.* created a cell permeable, fluorescently tagged derivative, PCI-33380 by attaching a bodipy-FL fluorophore to ibrutinib for in-gel fluorescence detection of

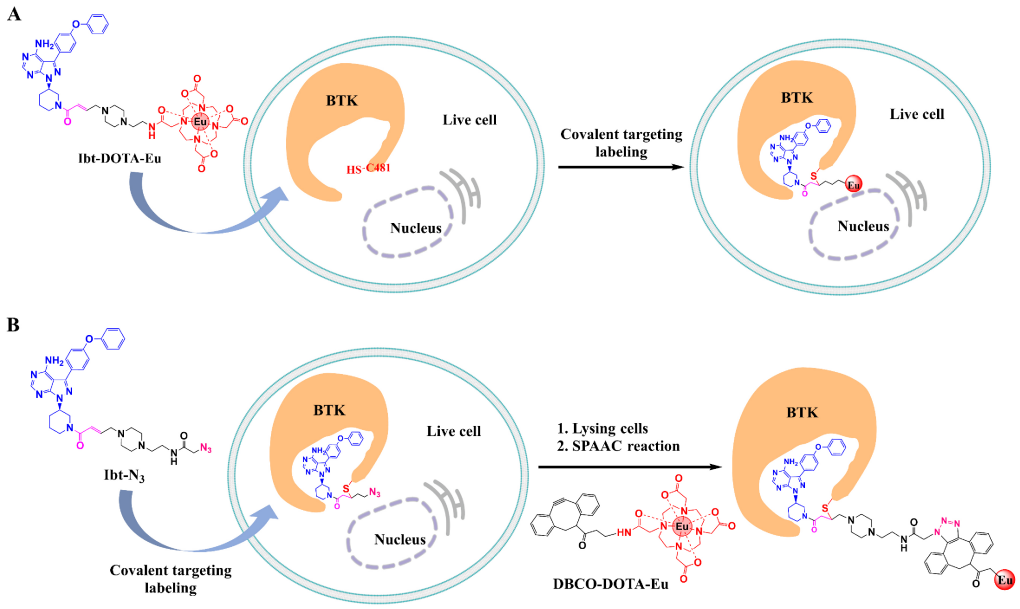

Scheme 1. Strategies designed for tagging Europium (Eu) to BTK in live cells. (A) A one-step strategy through using an DOTA-Eu (red ball) labeled ibrutinib probe (Ibt-DOTA-Eu) for directly attaching Eu to BTK in live cells. (B) A two-steps strategy through using an azido-modified ibrutinib probe (Ibt-N_3) for firstly attaching the azido group to BTK in live cell, and secondly DBCO-DOTA-Eu tagging via the specific strain-promoted azide-alkyne cycloaddition (SPAAC) reaction.

BTK.[10] As an FDA approved covalent targeting drug for B-cell malignancies therapy, ibrutinib is able to specifically recognize the ATP binding pocket of BTK, and form stable complex with BTK through covalent reaction between its acrylamide group and thiol group of Cys481 of BTK.[16] Based on the similar principle, several fluorescent probes were designed by conjugating different fluorophores to ibrutinib for imaging or detection of BTK.[10-15] However, fluorescence assay usually suffers from shortcomings such as spectra overlapping, background spectral interferences, and fluorescence bleaching and quenching, which compromise its ability for accurate protein quantification. Precise quantification of BTK in live cells remains a challenge.

As a powerful technology that can precisely quantify elements with high sensitivity, inductively coupled plasma mass spectrometry (ICP-MS) has been recognized as an attractive tool for biomolecule quantification.[17-26] Thanks to its unique feature that the signal of an element is independent of its chemical form, i. e. either in a free state or tagged on a protein, a metal-labeled protein can be absolutely quantified by using only one element/isotope standard through species-unspecific isotope dilution (SUID) ICP-MS.[18,19] A series of chemically selective and biologically specific elements labeling strategies were developed for absolute quantification of a diverse range of biological molecules using HPLC/SUID-ICP-MS.[18-26]

With the advantages of minimal polyatomic interference, low background interference, and an ionization efficiency up to 100% in argon plasma, the detection limit of lanthanides in ICP-MS can be as low as pg/L, which make lanthanides extremely suitable for protein quantification.[18-23, 27-29] In order to label lanthanides onto protein, 1,4,7,10-tetraazacyclododecane-1,4,7,10-tetraacetic acid (DOTA), a macrocyclic chelator which can form extremely stable complexes with lanthanides, is widely utilized.[27-29]

Given the importance of BTK quantification in live cells, herein we aimed to develop an effective strategy enabling in situ BTK specific labeling, lanthanide tagging, and HPLC/SUID-ICP-MS quantification. Ibrutinib, the BTK covalent targeting drug, was chosen as the targeting molecule for BTK labeling. In this study, we design two strategies to attach Europium (Eu) to BTK in live cells (Scheme 1): 1) A one-step strategy through using an DOTA-Eu labeled ibrutinib probe (Ibt-DOTA-Eu) for directly attaching Eu to BTK in live cells (Scheme 1A); and 2) A two-steps strategy through using an azido-modified ibrutinib probe (Ibt-N_3) for firstly attaching the azido group to BTK in live cells, and secondly DBCO-DOTA-Eu tagging via the specific strain-promoted azide-alkyne cycloaddition (SPAAC) reaction (Scheme 1B). Afterwards, the content of BTK in live cells was obtained through quantifying the Eu that was labeled on BTK using HPLC/SUID-ICP-MS.

EXPERIMENTAL

Materials. Ibrutinib, 1-Ethyl-3-(3-dimethylaminopropyl) carbodiimide hydrochloride (EDC), N-hydroxysuccinimide (NHS), Sinapic acid (SA), O-(7-azabenzotriazol-1-yl)-N, N, N', N'-tetramethyluronium hexafluorophosphate (HATU), 2,5-Dihydroxybenzoic acid were purchased from Aladdin (Shanghai,

China). Enriched ^{153}Eu isotope (99.99%) was purchased from Cambridge Isotope Laboratory (Andover, MA, USA). Azidoacetic Acid NHS Ester, BTK inhibitor 1 (R enantiomer), N, N-Diisopropylethylamine (DIPEA) and dibenzocyclooctyne-amine were purchased from Macklin (Shanghai, China). 1,4,7,10-Tetraazacyclododecane-1,4,7,10-tetraacetic acid (DOTA) was purchased from Confluore (Xian, China). 4-Bromocrotonic Acid was purchased from Energy Chemical (Anhui, China). 1-[2-(Boc-amino) ethyl] piperazine was purchased from Accela (Shanghai, China). Digitonin was purchased from Beyotime (Shanghai, China). Recombinant human BTK protein was purchased from Sino Biological (Beijing, China). RPMI 1640 medium, fetal bovine serum, penicillin/streptomycin, RIPA lysis buffer, Phosphatase inhibitor complex II, 1,4-dithiothreitol (DTT), Phenylmethyl sulfonyl fluoride (PMSF), Protein Quantification Kit (BCA assay) were purchased from Sangon (Shanghai, China). The B lymphocyte cell line Ramos was purchased from the American Type Culture Collection (ATCC, Manassas, American).

Instrumentations. Chromatographic separations were carried out on an HPLC system (LC-16P, Shimadzu, Kyoto, Japan) equipped with a Shimadzu SPD-16 UV detector. Products were characterized by Bruker Impact II electrospray ionization quadrupole time-of-flight mass spectrometer (ESI-Q-TOF-MS, Germany). ^{1}H- and ^{13}C-NMR spectra were collected on a Bruker Advance 500 (500 MHz) spectrometer. ICP-MS experiments were performed on a quadrupole-based inductively coupled plasma mass spectrometer (NEXION 2000, PerkinElmer, SCIEX, Canada).

Synthesis of compound c. 4-Bromocrotonic Acid (Compound a, 164 mg, 1 mmol) was dissolved in THF (5 mL). A solution of 1-[2-(Boc-amino) ethyl] piperazine (compound b, 229 mg, 1 mmol) and triethylamine (TEA, 0.42 mL, 3.0 mmol) in THF (2 mL) was added and the mixture was stirred overnight and concentrated under reduced pressure. The product c was used without further purification. ESI-MS (m/z): 314.1989 [M + H$^+$].

Synthesis of compound e. Triethylamine (0.25 mL, 1.75 mmol) was added to a solution of compound c (313 mg, 1.0 mmol) and HATU (190 mg, 0.5 mmol) in DMF (5 mL), after stirring at room temperature for 5 min, the solution of ibrutinib intermediate (Compound d, 100 g, 0.25 mmol) in DMF (2 mL) was added and the resulting mixture was stirred at room temperature overnight. EtOAc (25 mL) was added and then washed with brine, dried over $MgSO_4$, filtered, and concentrated in vacuo. The crude product was purified by column chromatography on silica gel (CH_2Cl_2/MeOH, 10:1) to afford product e (yield: 128 mg, 0.18 mmol, 75%). ESI-MS (m/z): 682.3791 [M + H$^+$]. ^{1}H NMR (500 MHz, $CDCl_3$-d_1) δ 8.35 (s, 1H), 7.64 (d, J = 8.6 Hz, 2H), 7.43 – 7.37 (t, 2H), 7.16 (dd, J = 15.6, 7.9 Hz, 5H), 6.88 – 6.75 (m, 1H), 6.50 – 6.34 (m, 1H), 5.60 (s, 2H), 5.05 (s, 1H), 4.86 (s, 2H), 4.53 (d, J = 13.2 Hz, 1H), 4.15 (q, J = 8.5, 7.1 Hz, 1H), 3.33 – 3.04 (m, 6H), 2.99 – 2.84 (m, 1H), 2.48 (dd, J = 14.4, 8.4 Hz, 9H), 2.25 (d, J = 12.1 Hz, 1H), 2.00 (s, 1H), 1.76 – 1.65 (m, 1H), 1.37 – 1.20 (m, 6H). ^{13}C NMR (125 MHz, MeOD-d_4) δ 166.20, 166.20, 165.98, 165.59, 158.51, 158.48, 158.48, 156.97, 156.57, 155.32, 155.28, 153.85, 141.01, 140.99, 140.62, 129.85, 129.70, 127.59, 123.70, 123.38, 123.26, 123.14, 119.14, 118.59, 97.82, 78.73, 58.82, 58.71, 57.17, 52.76, 42.33, 36.89, 29.66, 28.91, 27.38, 24.55, 22.83.

Synthesis of compound f. Compound e (200 mg, 0.29 mmol) was dissolved and stirred in 4.0 M HCl in dioxane (4 mL) for 2 h. The reaction mixture was filtered and the retained solids were washed with 3 portions of EtOAc and dried under reduced pressure. The product f was obtained without further purification as a white solid (162 mg, 0.28 mmol, 96%). ESI-MS (m/z): 582.3139 [M + H$^+$]. ^{1}H NMR (400 MHz, DMSO-d_6) δ 8.26(s, 1H), 7.68 (d, 2H), 7.42 (t, 2H),7.20–7.11 (m, 5H), 6.52 (t, 1H), 6.48–6.42 (m, 2H),5.88 (br s, 1H), 4.78–4.72 (m, 1H), 4.33 (d, 1H),4.01 (dt, 1H), 3.60–3.57 (m, 1H), 3.51 (t, ,1H), 3.27–3.18 (m, 1H), 3.10–3.04 (m, 6H), 2.42– 2.37 (m, 6H),2.21–2.17 (m, 1H), 2.03–1.96 (m, 1H), 1.70–1.59 (m, 1H). ^{13}C NMR (125 MHz, DMSO-d_6) δ 164.90, 158.66, 157.61, 156.75, 156.09, 154.44, 143.73, 130.57, 129.11, 128.41, 125.35, 124.25, 122.99, 119.43, 97.88, 70.26, 61.12, 59.22, 53.27, 46.20, 38.70, 38.57, 30.28, 29.48, 29.07, 28.83, 27.40, 23.73, 22.84, 22.54, 14.32, 11.25.

Synthesis of Ibt-DOTA. To a solution of DOTA (83 mg, 0.206 mmol) in 6 mL 1:2 DMF/H_2O was added triethylamine until pH was adjusted to 5-6. EDC (40 mg, 0.206 mmol) was added, and the solution was stirred for 5 min. Then NHS (24 mg, 0.206 mmol) was added to the solution at an ice bath, and stirred for additional 15 min. Additional compound f (60 mg, 0.103 mmol) was added and triethylamine was used to adjust pH to 7-8. After stirring at room temperature for 12 h, the crude product was further purified by HPLC to give product (Ibt-DOTA, 85 mg, 0.087 mmol, 85%) as white solids. ESI-MS (m/z): 968.5101 [M + H$^+$]. ^{1}H NMR (500 MHz, MeOD-d_4) δ 8.32 (s, 1H), 7.80 (d, 2H), 7.63 – 7.57 (t, 2H), 7.37 – 7.29 (m, 2H), 7.13 – 7.06 (m, 3H), 7.04 – 6.98 (m, 2H), 6.67 – 6.58 (m, 1H), 4.54 (d, J = 12.9 Hz, 1H), 4.17 (dd, J = 28.6, 12.8 Hz, 1H), 4.05 – 3.86 (m, 4H), 3.75 – 3.40 (m, 16H), 3.34 (s, 6H), 3.12 (dd, J = 13.1, 5.9 Hz, 9H), 2.47 (s, 2H), 2.29 (d, J = 12.5 Hz, 3H), 2.17 (m, J = 13.0, 4.1 Hz, 1H), 1.99 (s, 1H), 1.72 – 1.58 (m, 1H), 1.26 – 1.16 (m, 1H). ^{13}C NMR (125 MHz, MeOD-d_4) δ 176.60, 165.53, 162.89, 162.60, 162.32, 162.04, 158.72, 155.62, 155.62, 151.86, 151.02, 147.44, 147.44, 146.31, 146.31, 146.30, 130.23, 130.08, 130.06, 130.06, 130.03, 129.99, 125.08, 125.06, 125.06, 124.42, 124.38, 124.38, 119.73, 119.36, 119.32, 118.99, 118.97, 117.40, 115.08, 112.77, 112.76, 53.77, 53.77, 51.10, 51.10, 46.37, 46.37, 28.61, 28.61, 23.85, 23.84.

Synthesis of Ibt-DOTA-Eu. Ibt-DOTA was dissolved in ammonium acetate buffer (100 mM, pH 6.8), and then a 2-fold molar excess of $EuCl_3$ was added for the coordination of Eu^{3+} into DOTA moiety for 3 h at room temperature in the dark. The mixture

was purified by HPLC. ESI-MS (m/z): 1118.3244 [M + H^+].

Synthesis of Ibt-N_3. DIPEA was added to a solution of compound f (100 mg, 0.172 mmol) and azidoacetic NHS Ester (compound i, -51 mg, 0.258 mmol) in DMF (5 mL) until pH was adjusted to 7-8. after stirring at room temperature for 5 h, the mixture was purified by HPLC to give product (Ibt-N_3, 93 mg, 0.140 mmol, 81%) as white solids. ESI-MS (m/z): 665.3814 [M + H^+]. H NMR (500 MHz, MeOD-d4) δ 8.41 (s, 1H), 7.72 – 7.65 (d, 2H), 7.42 (t, J = 8.6, 7.4 Hz, 2H), 7.19 (m, J = 15.9, 8.1 Hz, 3H), 7.14 – 7.07 (m, 2H), 6.87 (d, J = 15.1 Hz, 1H), 6.70 (q, J = 7.8, 7.1 Hz, 1H), 4.57 (dd, J = 12.9, 4.1 Hz, 1H), 4.23 (dt, J = 8.6, 4.4 Hz, 1H), 4.04 (dd, J = 11.2, 7.0 Hz, 1H), 3.94 (d, J = 5.1 Hz, 3H), 3.63 (d, J = 7.0 Hz, 2H), 3.54 (dt, J = 12.5, 7.1 Hz, 3H), 3.41 (d, J = 21.9 Hz, 1H), 3.26 (s, 2H), 3.22 (s, 1H), 3.15 – 2.97 (m, 6H), 2.43 – 2.34 (m, 1H), 2.27 (dd, J = 9.0, 4.4 Hz, 1H), 2.15 – 2.02 (m, 1H), 1.80 – 1.66 (m, 1H). 13C NMR (125 MHz, MeOD-d4) δ 169.80, 165.48, 165.42, 161.32, 161.05, 159.18, 156.34, 156.34, 151.93, 147.02, 146.90, 129.94, 129.90, 129.75, 129.75, 125.91, 125.90, 123.90, 119.29, 119.29, 118.70, 57.18, 56.01, 52.99, 51.59, 50.78, 50.04, 49.96, 45.82, 34.57, 29.32, 29.24, 24.33, 22.81.

Synthesis of DBCO-DOTA-Eu. To a solution of DOTA (compound g, 104 mg, 0.258 mmol) and EDC (99 mg, 0.516 mmol) in 5 mL DMF were added DIPEA until pH was adjusted to 7-8, and dibenzocyclooctyne-amine (compound k, 47 mg, 0.172 mmol) was added. After stirring at room temperature for 6 h, the crude product was further purified by HPLC. All the solid was dissolved in ammonium acetate buffer (50mM, pH 6.8), and then a 2-fold molar excess of $EuCl_3$(189 mg, 0.516 mmol) was added for the coordination of Eu^{3+} into DOTA moiety for 4 h at room temperature. The mixture was further purified by HPLC to give product (DBCO-DOTA-Eu, 93 mg, 0.114 mmol, 66%) as white solids. ESI-MS (m/z): 813.4156 [M + H^+].

Cell culture and probe treatment. Ramos cells were cultured in RPMI 1640 medium with 10% fetal bovine serum (FBS) and 1% penicillin/streptomycin at 37 ºC in a humidified incubator with 5% CO_2. Probe (Ibt-DOTA-Eu, Ibt-N_3) was dissolved in dimethyl sulfoxide (DMSO) to prepare 20.0 mM stock solution and further diluted with the culture medium to the desired concentration before being added to the culture media.

Cell viability and uptake assays. The cytotoxic effects of probes were assessed by Cell Counting Kit-8 (CCK-8). The cells were seeded into the wells of the 96-well plates at densities of 10000 cells in 90 μL cell culture media for 12 h. Then incubated for 72 h upon different concentrations of probes and ibrutinib (0.1% DMSO), and CCK-8 solution were added (10 μL/ well). After 4 h additional incubation, the absorbance values of each well were recorded using a microplate reader at 450 nm.

Cell uptake assays of probe Ibt-DOTA-Eu. Ramos cells were seeded into the wells of the plates at densities of 5×10^6 cells in 2 mL cell culture media, and treated with the indicated concentrations of Ibt-DOTA-Eu (DMSO, 0.1%) for 24 h. Then collect the culture media and the cells were washed three times with HEPES buffer. The cell pellets and the culture media were digested with 10% HNO_3 in a 65 °C water bath overnight. The solution was finally diluted five times and filtered and measured by ICPMS.

BTK occupancy assay. Ramos cells (5×10^6) were pre-incubated with increasing concentrations of probes (0.1% DMSO) for 1 h, then the cells were washed three times with HEPES buffer, and subsequently cells were labelled with 2 μM of a fluorescence-tagged derivative of ibrutinib (probe PCI-33380) for 1 h at 37°C. After washed with HEPES buffer, cells were lysed in RIPA buffer. The lysates were removed by centrifugation at 13000 g for 10 min and quantified by BCA assay. Finally analyzed by SDS-polyacrylamide gel electrophoresis (SDS-PAGE) and fluorescence gel scanning using a GE scanner.

Species-Unspecific Isotope Dilution HPLC/ICPMS (HPLC/SUID-ICP-MS). Separation of Eu-labeled protein was carried out on a Waters E2695 LC system (Waters, Massachusetts, USA) with A Zorbax 300SB C18 column (1.0 I.D. × 150 mm length; particle size, 3.5 μm). The gradient elution program was as follows: The 95% mobile phase A (0.1% TFA in ultrapure water) was maintained for 5 min, then mobile phase B (0.1% TFA in ACN) was increased from 5% to 40% in 5 min, then mobile phase B was increased from 40% to 60% in 20 min, then increased from 60% to 70% in 20 min with a flow rate of 0.05 mL min^{-1}. The effluent from the column was mixed with the enriched ^{153}Eu spike solution and continuously pumped by a syringe pump (Cole-Parmer, East Bunker Court Vernon Hills, IL) through a four-way connector, while ultrapure water (0.9 mL min-1) was introduced continuously to mitigate the effect of increasing the ACN in the mobile phase on the plasma stability and ionization efficiency. The online isotope ratio of ^{153}Eu to ^{151}Eu was monitored using an A quadrupole-based inductively coupled plasma mass spectrometer (ICP-MS) (NEXION 2000, PerkinElmer, SCIEX, Canada) equipped with a concentric pneumatic nebulizer and a cyclonic spray chamber. The ICPMS operational parameters were as follows: nebulizer gas, 1.0 L min-1; auxiliary gas, 1.2 L min-1; plasma gas, 15 L min-1; RF power, 1600 W; dwell time, 100 us.

$$MF_{sample}(t) = MF_{spike}\frac{M_{sample}}{M_{spike}}\frac{\left(h_{spike}^{151} - h_{spike}^{153}R_{sample}(t)\right)}{\left(h_{sample}^{153}R_{sample}(t) - h_{sample}^{151}\right)}$$

The online-measured ^{151}Eu/^{153}Eu isotope chromatograms were transformed into Eu mass flow chromatogram following the isotope dilution formula shown below:

On-line isotope dilution formula used for transforming ^{151}Eu and ^{153}Eu isotope chromatograms into Eu mass flow chromatogram.

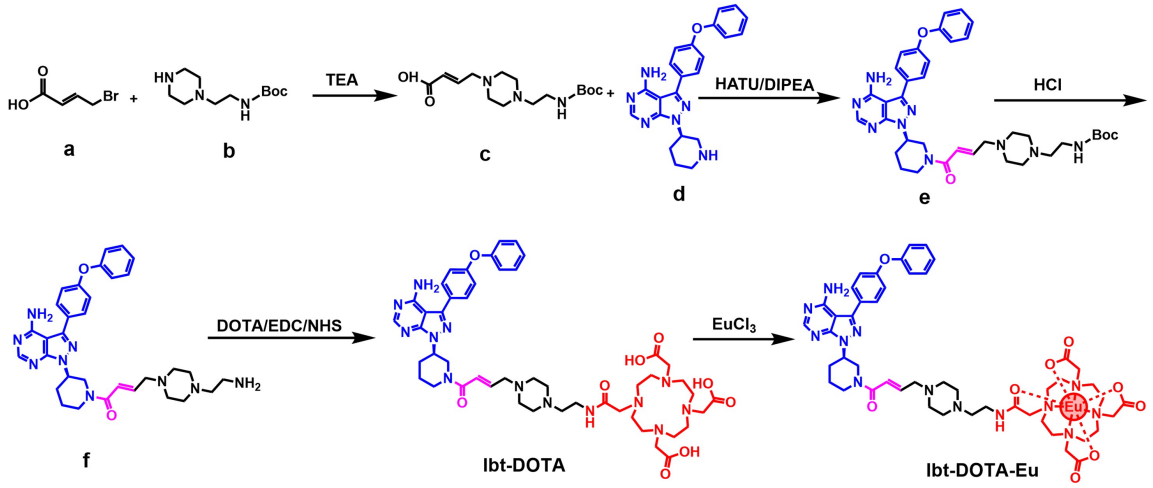

Fig. 1 Synthetic route of Ibt-DOTA-Eu.

MF_{sample} and MF_{spike} denote the mass flow of Eu of the sample and spiked solution. M_{sample} and M_{spike} denote the atomic mass of Eu in the sample and the spike solution, and $h_{sample}^{isotope}$ and $h_{spike}^{isotope}$ denote the isotope abundance of the respective isotope in the sample and spike solution. R_{sample} (t) is the on-line-measured $^{151}Eu/^{153}Eu$ isotope ratio during HPLC/ICP-MS.

Quantification of BTK protein by HPLC/SUID-ICP-MS. Ramos cells (5×10^6) were pre-incubated with increasing concentrations of probes (0.1% DMSO) for 1 h, then the cells were washed three times with HEPES buffer. After cell counting, 25 μL/1×10^6 cells RIPA lysis buffer was added to Ramos cells. The precipitation was removed by centrifugation at 13000 g for 10 min. BTK standard protein that was labeled with Ibt-N_3 probe was first added into the lysates. 20 equivalent of DBCO-DOTA-Eu was added to react with BTK-Ibt-N_3 for 2 h and excess probes were removed by ultrafiltration. Finally, Eu-tagged BTK were quantified through HPLC/^{153}Eu-SUID-ICP-MS. The SPACC labeling efficiency was finally obtained by dividing the quantitative result of Eu-tagged BTK into the theoretical content of the BTK standard protein.

RESULTS AND DISCUSSION

To test the feasibility of one step strategy for attaching Eu to BTK in live cells, we first designed and synthesized the Ibt-DOTA-Eu probe featuring an ibrutinib as the BTK reaction group and a DOTA-Eu complex as the ICPMS reporter, following the synthetic route outlined in Fig. 1. Detailed synthesis procedures were described in experimental section, and each compound was well characterized by HPLC-ESIMS and NMR (Figs. S1-S10). We verified the reactivity of Ibt-DOTA-Eu probe with recombinant BTK (Fig. 2) through in-gel fluorescence imaging. PCI-33380 (Fig. 2a), a Bodipy-FL fluorophore modified ibrutinib derivative was applied to detect the competitive binding of reporter to BTK.[10] As shown in Fig. 2b, PCI-33380 formed a stable adduct with BTK in the absence of Ibt-DOTA-Eu probe after 1 h incubation. Pre-treatment of BTK with increasing concentration of Ibt-DOTA-Eu probe gradually reduced the signal of PCI-33380 labeled BTK band. At a concentration of 20 nM, the PCI-33380 labeled BTK band was eliminated by Ibt-DOTA-Eu probe, indicating its high potency towards BTK protein (Fig. 2b). We further applied MALDI-MS to determine the molecular weight of BTK before and after Ibt-DOTA-Eu labeling. The obtained result indicated a 1:1 stoichiometry of Ibt-DOTA-Eu to BTK (Fig. 2c).

Encouraged by these results, we tried to apply Ibt-DOTA-Eu for in situ BTK labeling. However, we found that the BTK in live cells cannot be labeled by Ibt-DOTA-Eu, even when its concentration reached 200 nM (Fig. 2d), probably due to its low cellular uptake.

To verify this speculation, we compared the cytotoxicity of Ibt-DOTA-Eu probe with ibrutinib, and we found that Ibt-DOTA-Eu exhibits a much lower cytotoxicity to Ramos cells than that of ibrutinib (Fig. 2e), suggesting Ibt-DOTA-Eu probe could not penetrate cell membrane and induce cytotoxicity. Stronger evidence was obtained by directly determining the cellular uptake rate of Ibt-DOTA-Eu probe. We found that the content of Ibt-DOTA-Eu probe uptake by Ramos cells was 1% or lower than that in cell culture medium (Fig. 2f), confirming low cellular uptake as the reason for the low labeling efficiency of Ibt-DOTA-Eu to BTK in live cells. Therefore, this probe cannot be applied for directly Eu labeling of intracellular BTK.

To address the challenge of low cellular uptake rates of Ibt-DOTA-Eu, we switch over to the aforementioned two-steps labeling strategy. We first synthesized the azido-modified ibrutinib probe (Ibt-N_3) and the DBCO-DOTA-Eu (Fig. 3). Detailed synthesis procedures were described in experimental section, and

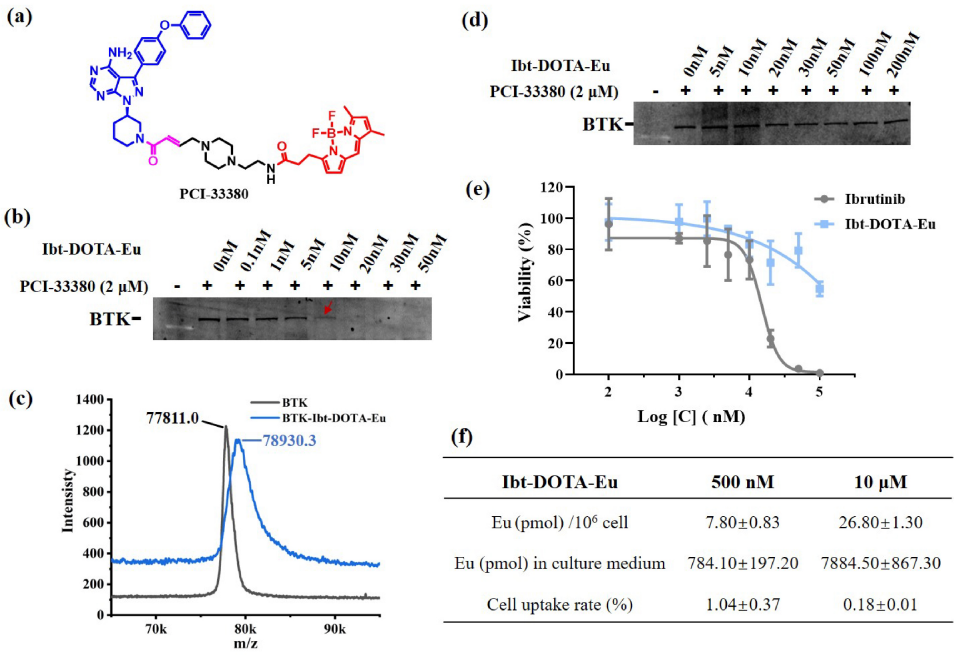

Ibt-DOTA-Eu	500 nM	10 μM
Eu (pmol) /10^6 cell	7.80±0.83	26.80±1.30
Eu (pmol) in culture medium	784.10±197.20	7884.50±867.30
Cell uptake rate (%)	1.04±0.37	0.18±0.01

Fig. 2 Evaluating the reactivity of Ibt-DOTA-Eu probe towards recombinant BTK protein and active BTK in live cells. (a) Structure of bodipy-labelled ibrutinib probe (PCI-33380). (b) Concentration-dependent binding between Ibt-DOTA-Eu and recombinant BTK by competitive fluorescent labeling of PCI-33380. The BTK labeled by PCI-33380 were determined by SDS-PAGE and in gel fluorescence scanning. (c) mass spectra of Ibt-DOTA-Eu labeled BTK determined by MALDI-TOFMS. (d) In-situ profiling the concentration-dependent binding between Ibt-DOTA-Eu and cellular BTK by competitive fluorescent labeling in live Ramos cells. (e) Dose-response curves of the viability of Ramos cells treated with varying concentrations of ibrutinib and Ibt-DOTA-Eu. IC_{50} values were obtained by fitting the dose-response curves of cell viability as a function of inhibitors' concentration. (f) Cellular uptake of Ibt-DOTA-Eu by Ramos cells. Cell uptake rates were calculated by comparing the concentration of probe that entered the cells with those in the cell culture medium.

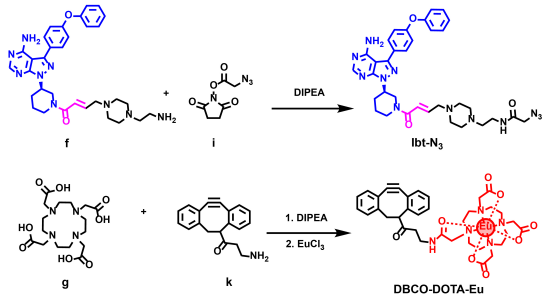

Fig. 3 Synthetic route of Ibt-N_3 and DBCO-DOTA-Eu.

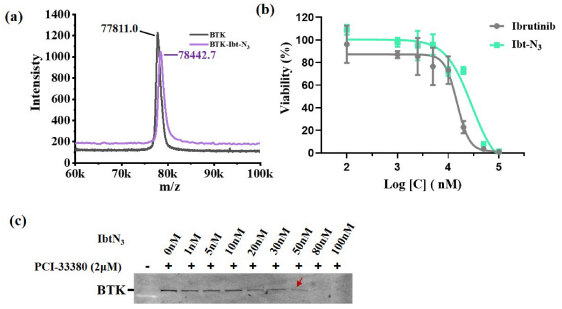

Fig. 4 The reactivity of the Ibt-N_3 probe towards the BTK protein. (a) Charge-to-mass ratio (m/z) shift diagram of Ibt-N_3 labeled recombinant BTK protein. (b) The proliferation inhibition of Ibrutinib and Ibt-DOTA-Eu toward Ramos cells detected by CCK-8 assay. (c) Occupancy test, assessed by the ability of BTK protein to bind to PCI-33380 in the presence of dose escalation of probe Ibt-N_3 in Ramos cell. The BTK labeled by PCI-33380 was determined by SDS-PAGE and in gel fluorescent scanning.

each compound was well characterized by HPLC-ESIMS and NMR (Figs. S11-S14). To determine the reactivity of Ibt-N_3 towards BTK, we determined the molecular weight of recombinant BTK before and after Ibt-N_3 labeling, which was found matched well with the theoretical value, indicating a precise 1:1 stoichiometry labeling of Ibt-N_3 to BTK (Fig. 4a).

To confirm that Ibt-N_3 addressed the issue of low cellular uptake encountered by Ibt-DOTA-Eu, we evaluated its cytotoxicity against Ramos cells. As expected, the IC50 value for Ibt-N_3 (15 μM) is comparable to that of ibrutinib (29 μM), indicating that the modification of azide group did not significantly alter the activity of Ibt-N_3 in terms of its ability to enter cells and bind to BTK protein (Fig. 4b). Moreover, we investigated the in-situ reactivity of Ibt-N_3 in live Ramos cells. As shown in Fig. 4c, Ibt-N_3 was found to label cellular BTK in a concentration dependent manner. When its concentration reached 80 nM, the intracellular BTK was completely labeled by Ibt-N_3, indicating that IbtN_3 has a better cell membrane permeability and can achieve in situ labeling of BTK in live Ramos cells, compared with Ibt-DOTA-Eu.

To achieve effective Eu-tagging to BTK, the efficiency of SPAAC reaction between BTK-Ibt-N_3 and DBCO-DOTA-Eu (Fig. 5a) should be carefully optimized in terms of the reaction time and the ratio of the two compounds. To optimize the SPACC efficiency between BTK-Ibt-N_3 and DBCO-DOTA-Eu, BTK standard protein

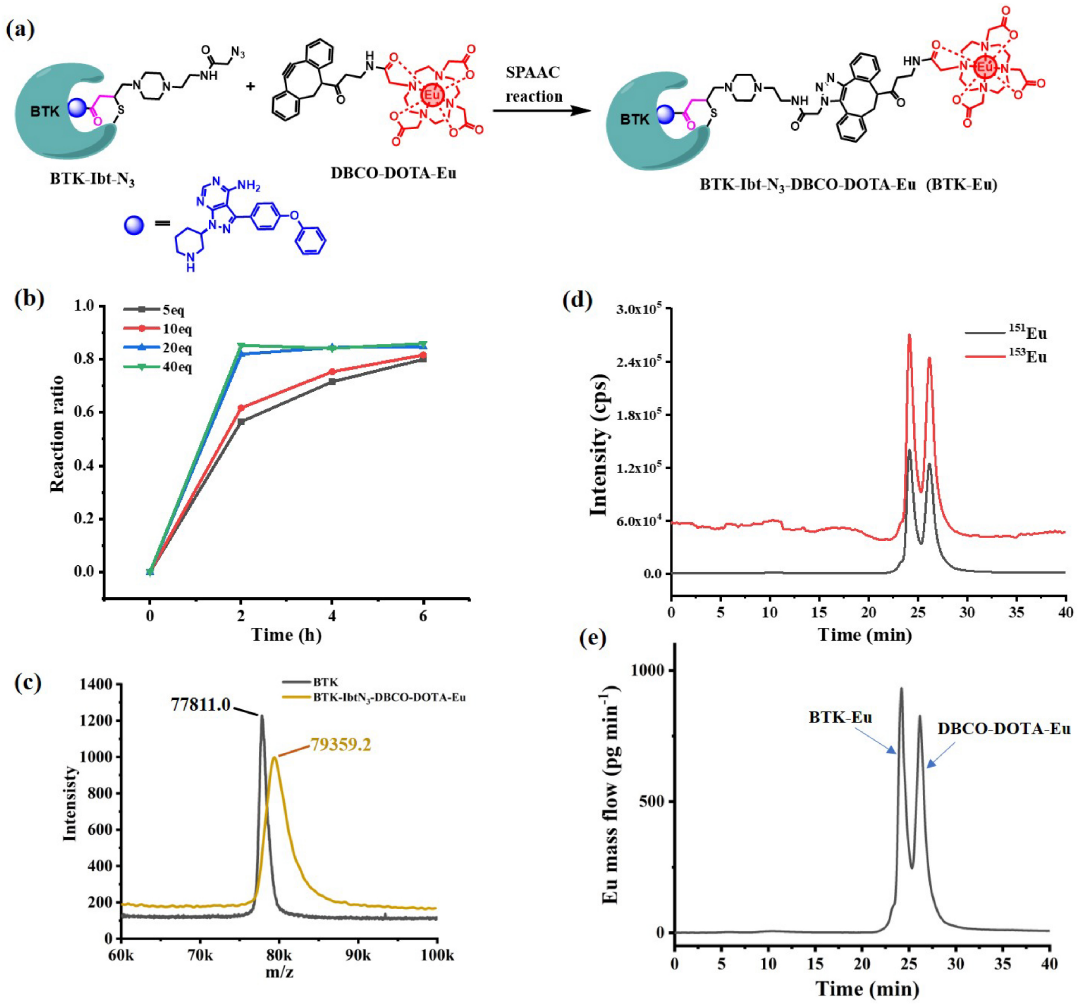

Fig. 5 (a) Schematic illustration of SPAAC reaction between BTK-Ibt-N_3 and DBCO-DOTA-Eu. (b) Optimization of the SPAAC reaction efficiency between BTK-Ibt-N_3 and DBCO-DOTA-Eu with varying ratio (DBCO-DOTA-Eu/IbtN$_3$: 5, 10, 20, and 40) under different reaction time. (c) Mass spectra of DBCO-DOTA-Eu labeled BTK-Ibt-N_3 as determined by MALDI-TOFMS. (d) ^{151}Eu and ^{153}Eu isotope chromatograms of DBCO-DOTA-Eu labeled BTK-Ibt-N_3 in cells lysate. Ramos cells were first incubated with Ibt-N_3, lysed, and then reacted with DBCO-DOTA-Eu. (e) Eu mass flow chromatogram transformed from (d).

that was labeled with Ibt-N_3 probe was first added into the cell lysates, followed by the addition of DBCO-DOTA-Eu to react with BTK-Ibt-N_3. The Eu-tagged BTK was then quantified by HPLC/SUID-ICP-MS. The labeling efficiency was finally obtained by dividing the quantitative result of Eu-tagged BTK into the theoretical content of the BTK standard protein. We found that when the quantity of DBCO-DOTA-Eu exceeds 20 equivalents to Ibt-N_3, the reaction reaches equilibrium in 2 hours (Fig. 5b). Under the optimized conditions of 20 equivalents DBCO-DOTA-Eu, BTK-Ibt-N_3 could be stability tagged with DBCO-DOTA-Eu with an 82% efficiency within 2 h. A 1:1 stoichiometry between BTK-Ibt-N_3 DBCO-DOTA-Eu was verified by MALDI-MS as shown in Fig. 5c.

Given the intracellular BTK proteins were labeled with Ibt-N_3 and tagged with DBCO-DOTA-Eu, we quantified the BTK protein in live Ramos cells using HPLC/^{153}Eu-SUID-ICP-MS. DBCO-DOTA-Eu labeled BTK-N_3 in cells lysate were separated on a C18 reverse phase column, and species-unspecific isotope dilution analysis was performed by mixing the ^{153}Eu-enriched spike solution with the HPLC effluent continuously, and both the ^{151}Eu and ^{153}Eu isotopes were monitored by ICPMS. As shown in Figs. 5d and 5e, the online-measured ^{151}Eu/^{153}Eu isotope chromatograms (Fig. 5d) were transformed into Eu mass flow chromatogram following the isotope dilution formula shown in EXPERIMENTAL section (Fig. 5e).[18,19] BTK-Eu is found to be the only protein peak detected by ICPMS, which indicate the high selectivity of DBCO-DOTA-Eu for labeling BTK-Ibt-N_3 in cell lysate. Although most of the excess DBCO-DOTA-Eu probe was removed by ultrafiltration, a small portion of DBCO-DOTA-Eu remained, whose retention time was close to that of BTK protein. To obtain the accurate protein quantification result, we used peak fitting algorithm of OriginPro software to mathematically separate the peaks of BTK-Eu and DBCO-DOTA-Eu into discrete areas.

By integrating the peak area and calculating based on the 82% reaction efficiency between BTK-Ibt-N_3 and DBCO-DOTA-Eu, the concentrations of BTK proteins were determined to be 61.28 ng/10^6 cells. To our knowledge, this is the first study realizing active BTK quantification in live cells by using covalent targeting drug mediated lanthanide labeling and ICP-MS.

CONCLUSION

In summary, we have designed and synthesized a cell permeable Ibt-N_3 probe, enabling BTK labeling in live cells and further facilitating Eu-tagging through the biorthogonal SPAAC reaction with DBCO-DOTA-Eu. This strategy effectively circumvents the issue of low cellular permeability of DOTA-Ln probe for direct BTK Eu-tagging in live cells. Active BTK within live cells was accurately quantified by using HPLC/SUID-ICP-MS. We believe the strategy established in this study can be extended to the quantification of other disease relevant kinase in live cells, which will prompt the application of ICP-MS in disease diagnosis and drug development.

ASSOCIATED CONTENT

Supporting information (Figs. S1−S14) is available at www.at-spectrose.com/as/home.

AUTHOR INFORMATION

Xiaowen Yan received his BSc in 2007 and PhD in 2012 from Xiamen University, and did postdoctoral research at University of Alberta from 2013 to 2019. He is currently an associate professor of analytical chemistry at Xiamen University. His research interests are mainly focused on the development of functional probes and approaches for elemental mass spectrometry-based bioanalysis, novel arsenic drugs, and targeted drug delivery. He has been working as member of editorial board for *Atomic Spectroscopy.*

Corresponding Author

* X. W. Yan

Email address: xwyan@xmu.edu.cn

†These authors contributed equally to this work.

Notes

The authors declare no competing financial interest.

ACKNOWLEDGMENTS

The authors gratefully thank the financial support from the National Key Research and Development Program of China (2022YFF0710200), the National Natural Science Foundation of China (22074127, 22193053), the Science and Technology Projects of Innovation Laboratory for Sciences and Technologies of Energy Materials of Fujian Province (IKKEM) (HRTP- [2022]-13), and the Fundamental Research Funds for the Central Universities (20720200073).

REFERENCES

1. Y. Aoki, K. J. Isselbacher, and S. Pillai, *Proc. Natl. Acad. Sci. U. S. A.*, 1994, **91**, 10606-10609. https://doi.org/10.1073/pnas.91.22.10606
2. W. N. Khan, *Immunol. Res.*, 2001, **23**, 147-156. https://doi.org/10.1385/IR:23:2-3:147
3. X. Wang, L. Kokabee, M. Kokabee, and D. S. Conklin, *Front. Cell Dev. Biol.*, 2021, **9**, 668996. https://doi.org/10.3389/fcell.2021.668996
4. T. Wen, J. Wang, Y. Shi, H. Qian, and P. Liu, *Leukemia*, 2021, **35**, 312-332. https://doi.org/10.1038/s41375-020-01072-6
5. A. B. Satterthwaite, H. Cheroutre, W. N. Khan, P. Sideras, and O. N. Witte, *Proc. Natl. Acad. Sci. U. S. A.*, 1997, **94**, 13152-13157. https://doi.org/10.1073/pnas.94.24.13152
6. W. H. Wilson, R. M. Young, R. Schmitz, Y. Yang, S. Pittaluga, G. Wright, C. J. Lih, P. M. Williams, A. L. Shaffer, J. Gerecitano, S. de Vos, A. Goy, V. P. Kenkre, P. M. Barr, K. A. Blum, A. Shustov, R. Advani, N. H. Fowler, J. M. Vose, R. L. Elstrom, T. M. Habermann, J. C. Barrientos, J. McGreivy, M. Fardis, B. Y. Chang, F. Clow, B. Munneke, D. Moussa, D. M. Beaupre, and L. M. Staudt, *Nat. Med.*, 2015, **21**, 922-926. https://doi.org/10.1038/nm.3884
7. S. Pal Singh, F. Dammeijer, and R. W. Hendriks, *Mol. Cancer*, 2018, **17**, 57. https://doi.org/10.1186/s12943-018-0779-z
8. S. F. H. Neys, R. W. Hendriks, and O. B. J. Corneth, *Front. Cell Dev. Biol.*, 2021, **9**, 668131. https://doi.org/10.3389/fcell.2021.668131
9. J. A. Di Paolo, T. Huang, M. Balazs, J. Barbosa, K. H. Barck, B. J. Bravo, R. A. Carano, J. Darrow, D. R. Davies, L. E. DeForge, L. Diehl, R. Ferrando, S. L. Gallion, A. M. Giannetti, P. Gribling, V. Hurez, S. G. Hymowitz, R. Jones, J. E. Kropf, W. P. Lee, P. M. Maciejewski, S. A. Mitchell, H. Rong, B. L. Staker, J. A. Whitney, S. Yeh, W. B. Young, C. Yu, J. Zhang, K. Reif, and K. S. Currie, *Nat. Chem. Biol.*, 2011, **7**, 41-50. https://doi.org/10.1038/nchembio.481
10. L. A. Honigberg, A. M. Smith, M. Sirisawad, E. Verner, D. Loury, B. Chang, S. Li, Z. Pan, D. H. Thamm, R. A. Miller, and J. J. Buggy, *Proc. Natl. Acad. Sci. U. S. A.*, 2010, **107**, 13075-13080. https://doi.org/10.1073/pnas.1004594107
11. A. Turetsky, E. Kim, R. H. Kohler, M. A. Miller, and R. Weissleder, *Sci. Rep.*, 2014, **4**, 4782. https://doi.org/10.1038/srep04782
12. X. Wang, N. Ma, R. Wu, K. Ding, and Z. Li, *Chem. Commun. (Camb)*, 2019, **55**, 3473-3476. https://doi.org/10.1039/c9cc01059a

13. E. Kim, K. S. Yang, R. H. Kohler, J. M. Dubach, H. Mikula, and R. Weissleder, *Bioconjug. Chem.*, 2015, **26**, 1513-1518. https://doi.org/10.1021/acs.bioconjchem.5b00152

14. J. Chen, X. Wang, F. He, and Z. Pan, *Bioconjug. Chem.*, 2018, **29**, 1640-1645. https://doi.org/10.1021/acs.bioconjchem.8b00137

15. N. Liu, S. Hoogendoorn, B. van de Kar, A. Kaptein, T. Barf, C. Driessen, D. V. Filippov, G. A. van der Marel, M. van der Stelt, and H. S. Overkleeft, *Org. Biomol. Chem.*, 2015, **13**, 5147-5157. https://doi.org/10.1039/c5ob00474h

16. Z. Pan, H. Scheerens, S. J. Li, B. E. Schultz, P. A. Sprengeler, L. C. Burrill, R. V. Mendonca, M. D. Sweeney, K. C. Scott, P. G. Grothaus, D. A. Jeffery, J. M. Spoerke, L. A. Honigberg, P. R. Young, S. A. Dalrymple, and J. T. Palmer, *Chem. Med. Chem.*, 2007, **2**, 58-61. https://doi.org/10.1002/cmdc.200600221

17. M. Wang, W. Feng, W. Lu, B. Li, B. Wang, M. Zhu, Y. Wang, H. Yuan, Y. Zhao, and Z. Chai, *Anal. Chem.*, 2007, **79**, 9128-9134. https://doi.org/10.1021/ac071483t

18. X. Yan, M. Xu, L. Yang, and Q. Wang, *Anal. Chem.*, 2010, **82**, 1261-1269. https://doi.org/10.1021/ac902163x

19. X. Yan, Y. Luo, Z. Zhang, Z. Li, Q. Luo, L. Yang, B. Zhang, H. Chen, P. Bai, and Q. Wang, *Angew. Chem. Int. Ed.*, 2012, **51**, 3358-3363. https://doi.org/10.1002/anie.201108277

20. X. Yan, L. Yang, and Q. Wang, *Anal. Bioanal. Chem.*, 2013, **405**, 5663-5670. https:// doi.org/10.1007/s00216-013-6886-1

21. R. Liu, X. Hou, Y. Lv, M. McCooeye, L. Yang, and Z. Mester, *Anal. Chem.*, 2013, **85**, 4087-4093. https://doi.org/10.1021/ac400158u

22. Y. Liang, X. Yan, Z. Li, L. Yang, B. Zhang, and Q. Wang, *Anal. Chem.*, 2014, **86**, 3688-3692. https://doi.org/10.1021/ac500123z

23. C. Liu, S. Lu, L. Yang, P. Chen, P. Bai, and Q. Wang, *Anal. Chem.*, 2017, **89**, 9239-9246. https://doi.org/10.1021/acs.analchem.7b02016

24. Z. Liu, X. Li, G. Xiao, B. Chen, M. He, and B. Hu, *TRAC-Trend. Anal. Chem.*, 2017, **93**, 78-101. https://doi.org/10.1016/j.trac.2017.05.008

25. C. Ji, Y. Liang, F. Ge, L. Yang, and Q. Wang, *Anal. Chem.*, 2019, **91**, 7032-7038. https://doi.org/10.1021/acs.analchem.9b01662

26. H. Du, P. Yang, L. Xia, J. Chen, and X. Hou, *TRAC-Trend. Anal. Chem.*, 2024, **172**, 117552. https://doi.org/10.1016/j.trac.2024.117552

27. X. Yan, L. Yang, and Q. Wang, *Angew. Chem. Int. Ed.*, 2011, **50**, 5130-5133. https://doi.org/10.1002/anie.201101087

28. G. Han, S. Zhang, Z. Xing, and X. Zhang, *Angew. Chem. Int. Ed.*, 2013, **125**, 1506-1511. https://doi.org/10.1002/ange.201206903

29. G. Schwarz, L. Mueller, S. Beck, and M. W. Linscheid, *J. Anal. At. Spectrom.*, 2014, **29**, 221-233. https://doi.org/10.1039/C3JA50277E